

# Switch Semi-Active Control of the Floating Raft Vibration Isolation System

Zeyu Weng\* – Shengli Liu – Teqi Xu – Xiaoyu Wu – Zhe Wang – Jie Tang  
Zhejiang University of Technology, College of Mechanical Engineering, China

*Switch semi-active control is introduced to improve the performance of the floating raft vibration isolation system on isolating vibration in the vicinity of the resonance frequency. A switch-controllable linear damper based on the electromagnetic damping principle is developed, whose characteristic parameters are obtained by experiment. The dynamic model of a semi-active control floating raft vibration isolation system is established, and two switch control algorithms are proposed. Algorithm 1 aims to minimize the kinetic energy of the raft, and Algorithm 2 balances minimizing the kinetic energy of the raft and minimizing the input energy of the system. The simulations of the original system, the system with the controllable damper, and the system with the damper controlled by the algorithms are carried out. The vibration acceleration responses of the foundation of the systems are used to evaluate the vibration isolation effect. The results show that the switching semi-active control using Algorithms 1 and 2 can significantly suppress the vibration of the system near the resonance frequency. Finally, the test platform of the switch's semi-active controlled floating raft vibration isolation system is built, and the simulation results are verified by the experimental result.*

**Keywords:** floating raft, semi-active control, vibration isolation, switch algorithm

## Highlights

- Two semi-active control algorithms for floating raft vibration isolation systems are proposed.
- Applying these two semi-active control algorithms can improve the vibration isolation performance of the floating raft isolation system.
- Two algorithms have different effects at different external excitation frequencies.

## 0 INTRODUCTION

As an extension of the double-layer vibration isolation system with multiple vibration sources, the floating raft vibration isolation system is widely used in the vibration isolation design of ship power units due to its good overall performance on vibration isolation [1]. However, the system has a poor isolation effect at low frequencies, especially near the system's resonance frequency, which may even amplify the vibration. Increasing the damping of the system is an effective method of suppressing resonance, and larger damping leads to a better suppression effect, but it affects the vibration isolation effect at middle and high frequencies. Using a switch-controllable damper and applying switch semi-active control technology on a floating raft vibration isolation system can effectively solve this problem.

The basic modes of vibration control include passive control, active control, and semi-active control. Compared with passive control, active control generally has a better effect and better adaptability [2] to [5]. However, it has higher requirements on the controllers and a limited effective control frequency band. Moreover, the stability and reliability of the system are difficult to guarantee. Once the vibration isolation system fails, the active control may amplify

the vibration and even destroy the entire system. As a result, the active control technology cannot be widely used in engineering applications. Alternatively, semi-active control is used since it has a control effect close to that of active control, as well as advantages of lower energy consumption and better system stability and reliability. After failure, the system will degenerate into an ordinary floating raft vibration isolation system, which still isolates the vibration to some extent during the normal operation of the whole system.

Semi-active control on the vibration isolation system is essentially a kind of parameter control. According to the change of system input and the requirements of system output, the stiffness and damping of the system are adjusted by an appropriate control algorithm in real-time so that the vibration characteristics of the system can be improved. At present, semi-active control technology has been widely used in vehicle suspensions and seismic resistance of buildings [6] and [7]. For the floating raft vibration isolation system, Sun [8] studied the isolation performance of a semi-active dynamic vibration absorber in a floating raft system under multi-frequency excitation. Chen Dayue's team [9] and [10] studied the vibration isolation characteristics of the floating raft isolation system under fuzzy control

and a synovial-film variable structure algorithm based on the ER damper. The results showed that different control algorithms could effectively improve the vibration isolation performance of the floating raft isolation system. The damper of the floating raft isolation system can be adjusted according to different requirements by using the methods of continuous semi-active control. This method has great potential. However, the adjustment range of the damper is only up to several times (generally no more than 10 times), and it is challenging to design an ideal control strategy due to the nonlinear damping characteristic; these factors limit its more comprehensive application. Switch semi-active control switches the state of a controllable damper on and off to improve the performance of vibration isolation. The control algorithm is simple and easy to operate, so the control system has high reliability. More importantly, the damping of the switch-controllable damper developed by our institute has strictly linear characteristics, the response time is down to milliseconds, and the damping can be adjusted up to tens of times. The experiments show that these characteristics and technical specifications are far superior to the existing dampers or controllable dampers that have been developed by some scholars, which guarantees the performance and reliability of semi-active control.

To summarize, it is of great significance to apply the switch semi-active control technology on the floating raft vibration isolation system with the self-developed switch-controllable damper. In this paper, we first characterize the damping properties of the developed controllable damper. Then, two switching-control algorithms are proposed to suppress the transmission of vibration from the unit to the foundation. Finally, using the acceleration response of the foundation as evaluation parameters, the effectiveness of the two algorithms is proved by simulation and experiment.

## 1 EXPERIMENTAL STUDY ON THE PERFORMANCE OF SWITCH-CONTROLLABLE LINEAR DAMPER

Properties characterizing the damping performance of the switch-controllable damper include the indicator, velocity, and response time, which is the key component to realize the semi-active control of the floating raft isolation system, and its performance determines the control effect. We independently developed the switch-controllable damper based on the electromagnetic damping principle. The control voltage is 24 V, direct current (DC). It has two states (on and off) corresponding to whether it is powered or not. When powered, the moving conductor and magnetic pole of the damper produce electromagnetic resistance and maintain a high damping value. Otherwise, it does not produce electromagnetic resistance, and the damper maintains a low damping value.

We carried out these tests on MTS849 Shock Absorber Test System (MTS Industrial Systems CO.LTD, USA) as shown in Fig. 1.



Fig. 1. MTS849 shock absorber performance test device used in the performance test

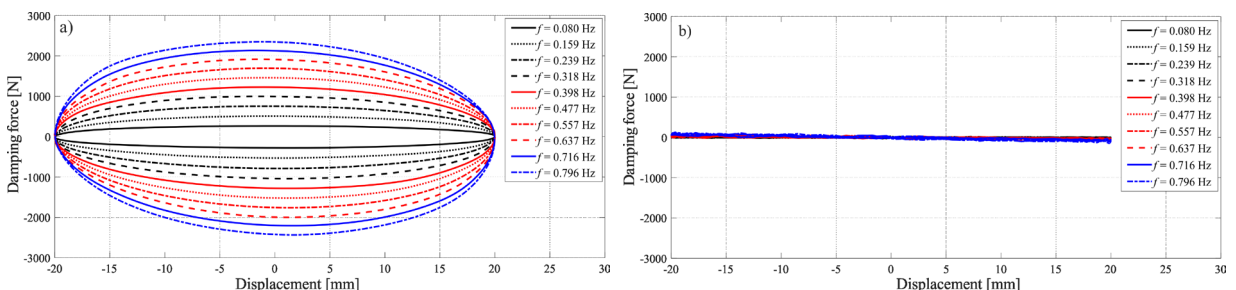
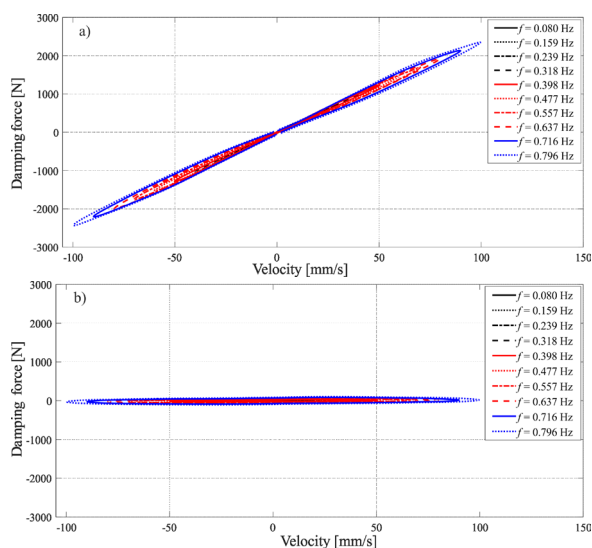


Fig. 2. Indicator diagram of the switch-controllable linear damper in different state, the curves show the relationship between damping force and displacement, the  $f$  in the tag represents the frequency at which the damper operates; a) on state, and b) off state

The indicator diagrams of the on and off states of controllable damper are shown in Fig. 2, where Fig 2a is for the on state and Fig. 2b is for off state. The curve family in Fig. 2 shows the relationship between the damping force generated by the damper and the motion displacement under different working frequencies. The curves in Fig. 2a are smooth, and the enclosed area is full, indicating that the damper can effectively absorb vibration energy when it is powered. The area enclosed by the curves in Fig. 2b is close to zero, indicating that the damper absorbs little vibration energy when it is not powered.



**Fig. 3.** Velocity characteristic curve of the switching-controllable linear damper in different state, the curves show the relationship between damping force and velocity, the  $f$  in the tag represents the frequency at which the damper operates; a) on state, and b) off state

The curves of the velocity characteristics of controllable damper are shown in Fig. 3; Fig. 3a is for the on state and Fig. 3b for off state. In Fig. 3, the curves show the relationship between the damping force generated by the damper and the motion velocity under different working frequency of the damper. The on state of the switch-controllable damper has great linear damping force velocity characteristics, meaning that the damper behaves as the pure viscous damper, and its damping coefficient is the slope of the curve. At the same time, the damping in the off state of the switch-controllable damper approaches a small constant.

It can be seen from the damper velocity characteristic curve that the damping characteristic of the controllable damper has obvious linear properties. We perform linear fitting on the speed characteristic

data of the controllable damper in different states, and obtain that the damping coefficient of the controllable damper in the on state is  $24050 \text{ N}\cdot\text{m}^{-1}\cdot\text{s}$ , and the damping coefficient in the off state is  $1050 \text{ N}\cdot\text{m}^{-1}\cdot\text{s}$ .

In addition, the response time of the switch-controllable damper can be obtained by comparing the electrical signals controlling the damper and damping force output responses.

The characterizing parameters of the controllable damper obtained through the tests are shown in Table 1.

**Table 1.** Performance parameters of switch damper

Parameter	Numerical value	
	On state	Off state
Damping coefficient [ $\text{N}\cdot\text{m}^{-1}\cdot\text{s}$ ]	$2.405 \times 10^4$	1050
Power consumption [W]	9.12	0
Response time [ms]	22	18
Working voltage DC [V]	24	
Quality [kg]	6.3	
Working distance [mm]	$\pm 32$	

## 2 DYNAMIC MODEL

According to the magnitude of the foundation stiffness, two kinds of dynamic models of vibration isolation systems are commonly used: one with rigid foundation and the other with flexible foundation. In the analysis of the vibration isolation system, some scholars neglected the flexibility of the foundation and assumed infinite stiffness, thus established the rigid foundation model as shown in Fig. 4.

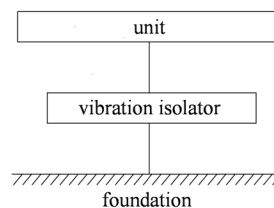


**Fig. 4.** Simplified model of rigid foundation isolation system, here the stiffness of the foundation is assumed to be infinite

However, from the research of Hamme [11] and Sykes [12], we know this simplification usually leads to some error. In addition, the vibration response on the foundation cannot be reflected in the model of rigid foundation, it is impossible to evaluate the isolation effect by foundation acceleration response. In conclusion, it is crucial to establish an analytical model of the floating raft isolation system with flexible foundation, as shown in Fig. 5.

The semi-active controlled floating raft vibration isolation system consists of four parts: a unit, an elastic element, a controllable damper, a raft, and the foundation. As shown in Fig. 5,  $F$  represents the excitation force applied on the unit;  $m_1$ ,  $m_2$  and  $m_3$  are the equivalent mass of the unit, raft and foundation respectively;  $c_1$  and  $k_1$  are the equivalent damping and stiffness between the unit and raft;  $c_2$  and  $k_2$  are the equivalent damping and stiffness between the raft and foundation;  $c_3$  and  $k_3$  and are the equivalent damping and stiffness of foundation;  $c_4$  is the damping of the controllable damper,  $c_{on}$  is the high damping at on state while  $c_{off}$  is low damping at off state;  $x_1$ ,  $x_2$  and  $x_3$  are the displacement responses of the unit, raft and foundation respectively,  $v_1$ ,  $v_2$  and  $v_3$  are the velocity responses,  $a_1$ ,  $a_2$  and  $a_3$  are the acceleration responses.

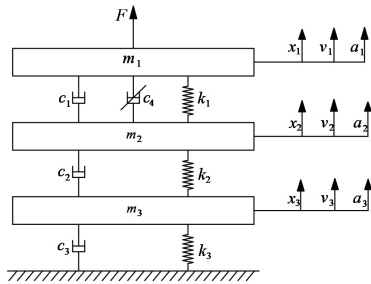


Fig. 5. Dynamic model of semi-active control floating raft isolation system

The dynamical equation corresponding to the model can be expressed as Eq. (1).

$$\begin{bmatrix} m_1 & 0 & 0 \\ 0 & m_2 & 0 \\ 0 & 0 & m_3 \end{bmatrix} \begin{bmatrix} \ddot{x}_1 \\ \ddot{x}_2 \\ \ddot{x}_3 \end{bmatrix} + \begin{bmatrix} c_1 + c_4 & -c_1 & 0 \\ -c_1 - c_4 & c_2 & -c_2 \\ 0 & -c_2 & c_3 \end{bmatrix} \begin{bmatrix} \dot{x}_1 \\ \dot{x}_2 \\ \dot{x}_3 \end{bmatrix} + \begin{bmatrix} k_1 & -k_1 & 0 \\ -k_1 & k_1 + k_2 & -k_2 \\ 0 & -k_2 & k_2 + k_3 \end{bmatrix} \begin{bmatrix} x_1 \\ x_2 \\ x_3 \end{bmatrix} = \begin{bmatrix} F \\ 0 \\ 0 \end{bmatrix}, \quad (1)$$

which shows that the damping matrix of the system can be changed by adjusting the damping of the controllable damper  $c_4$ , thus makes effect on the vibration response of the floating raft vibration isolation system.

### 3 ALGORITHMS

To realize switch semi-active control of the floating raft vibration isolation system and improve its effect, two switch control algorithms named Algorithms 1 and 2 are proposed in this paper.

#### 3.1 Algorithm 1

The goal of Algorithm 1 is to minimize the kinetic energy transmitted to the raft by adjusting the elastic energy absorbed or released by the elastic element.

The vibrational energy transited to the system by the excitation force transforms into the kinetic energy of the mass element, the potential energy of the elastic element, and the energy consumed by the damping element. The damping element consumes the energy, while the kinetic energy of the mass element and the potential energy of the elastic element are transformed mutually. More specifically, the vibration energy transmitted to the system is simultaneously converted into the kinetic energy of unit, the potential energy of the elastic element between unit and raft, the energy consumed by the damping element between unit and raft, and the kinetic energy of raft. Among them, the increase of kinetic energy of raft leads to the increase of the energy transmitted to the foundation, which exacerbates the vibration of the foundation. The kinetic energy of the raft can be reduced as much as possible by controlling the damping force. When the elastic element absorbs energy, the controllable damper is switched to the off state to minimize the damping value, which makes the elastic element absorb more energy and thus reduces the energy transited to the raft. When the elastic element releases energy, the controllable damper is switched to the on state to maximize the damping value, which makes the damper consume more energy and thus reduces the energy released from the spring to the raft.

According to the displacement and velocity differences between the unit and raft, the motion of the floating raft vibration isolation system can be divided into four states as shown in Fig. 6, where dotted lines are the equilibrium positions of the unit and raft.

In Fig. 6a, the displacement difference between the unit and raft is positive ( $x_1 - x_2 > 0$ ), which means the spring element between unit and raft is elastically restored; the velocity difference is positive ( $v_1 - v_2 > 0$ ), which means the displacement difference between the two will increase. In this state, the elastic element absorbs energy and the controllable damper should be in the off state.

In Fig. 6b, the displacement difference between the unit and the raft is positive ( $x_1 - x_2 > 0$ ), which means the spring element between the unit and raft is elastically restored; the velocity difference is negative ( $v_1 - v_2 < 0$ ), which means the displacement difference between the two will decrease. In this state, the elastic element releases energy and the controllable damper should be in the on state.

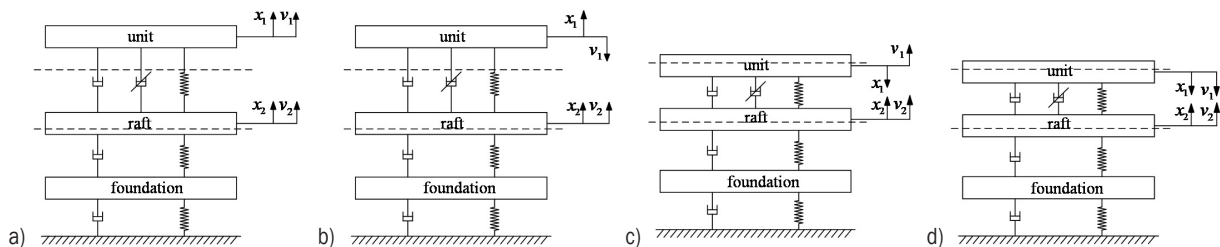


Fig. 6. System state decided by the displacement difference and velocity difference; a), b), c) and d) are explained in the article

In Fig. 6c, the displacement difference between the unit and the raft is negative ( $x_1 - x_2 < 0$ ), which means the spring element between unit and raft is compressed; the velocity difference is positive ( $v_1 - v_2 > 0$ ), which means the displacement difference between the two will increase. In this state, the elastic element releases energy and the controllable damper should be in the on state.

In Fig. 6d, the displacement difference between the unit and the raft is negative ( $x_1 - x_2 < 0$ ), which means the spring element between unit and raft is compressed; the velocity difference is negative ( $v_1 - v_2 < 0$ ), which means the displacement difference between the two will decrease. In this state, the elastic element absorbs energy and the controllable damper should be in the off state.

Based on the analysis of each state above, the control law of Algorithm 1 can be expressed as

$$c_4 = \begin{cases} c_{off} & (x_1 - x_2) > 0, (v_1 - v_2) > 0 \\ c_{on} & (x_1 - x_2) > 0, (v_1 - v_2) < 0 \\ c_{on} & (x_1 - x_2) < 0, (v_1 - v_2) < 0 \\ c_{off} & (x_1 - x_2) < 0, (v_1 - v_2) > 0 \end{cases} P_F = F \cdot v_1, \quad (2)$$

which can be simplified as

$$c_4 = \begin{cases} c_{off} & (x_1 - x_2) \cdot (v_1 - v_2) \geq 0 \\ c_{on} & (x_1 - x_2) \cdot (v_1 - v_2) < 0 \end{cases} \quad (3)$$

### 3.2 Algorithm 2

Algorithm 2 aims to makes the balance on minimizing the input energy of the system and minimizing the kinetic energy of the raft.

The power of the excitation force on the unit can be expressed as

$$P_F = F \cdot v_1, \quad (4)$$

the controllable damping force also works on the unit and its power can be expressed as

$$P_{c1} = c_4 \cdot (v_2 - v_1) \cdot v_1. \quad (5)$$

If both  $P_F$  and  $P_{c1}$  are positive, then

$$P_F \cdot P_{c1} = F \cdot c_4 \cdot (v_2 - v_1) \cdot v_1^2 \geq 0, \quad (6)$$

that is

$$F \cdot (v_2 - v_1) \geq 0. \quad (7)$$

The excitation force inputs energy to the system and the controllable damping force will exacerbate this input, the controllable damper should be in the off state to reduce the input energy. If  $P_F$  is positive while  $P_{c1}$  is negative then

$$F \cdot c_4 \cdot (v_2 - v_1) < 0, \quad (8)$$

that is

$$F \cdot (v_2 - v_1) < 0. \quad (9)$$

The excitation force inputs energy to the system and the controllable damping force will attenuate this input, so the controllable damper should be in the on state to reduce the input energy. If  $P_F$  is negative while  $P_{c1}$  is positive then

$$F \cdot c_4 \cdot (v_2 - v_1) < 0, \quad (10)$$

that is

$$F \cdot (v_2 - v_1) < 0. \quad (11)$$

The excitation force absorbs energy from the system and the controllable damping force will enhance the absorption, so the controllable damper should be in the on state to increase the energy absorption. If both  $P_F$  and  $P_{c1}$  are negative then

$$F \cdot c_4 \cdot (v_2 - v_1) \geq 0, \quad (12)$$

that is

$$F \cdot (v_2 - v_1) \geq 0. \quad (13)$$

The excitation force absorbs energy from the system and the controllable damping force will attenuate the absorption, so the controllable damper

should be in the off state to increase the energy absorption.

In short, when the excitation force and the controllable damping force are in the same direction, the controllable damper should be in a low damping state; while in the opposite direction, the controllable damper should be in a high damping state. The damping expression of the controllable damper is

$$c_4 = \begin{cases} c_{off} & F \cdot (v_2 - v_1) \geq 0 \\ c_{on} & F \cdot (v_2 - v_1) < 0 \end{cases} \quad (14)$$

Both Algorithm 1 and Eq. (14) give the expressions of the controllable dampers, which are incompatible. Algorithm 2 combines Algorithm 1 with Eq. (14). That is: if the control results of Algorithm 1 and Eq. (14) are consistent, then take the common result as the criterion and set the state of the controllable damper accordingly. Otherwise, the controllable damper is set to the active mode to consume more energy. In conclusion, the control law of Algorithm 2 can be expressed as

$$c_4 = \begin{cases} c_{off} & F \cdot (v_2 - v_1) \geq 0, (x_1 - x_2) \cdot (v_1 - v_2) \geq 0 \\ c_{on} & F \cdot (v_2 - v_1) < 0, (x_1 - x_2) \cdot (v_1 - v_2) < 0 \\ c_{on} & F \cdot (v_2 - v_1) \geq 0, (x_1 - x_2) \cdot (v_1 - v_2) < 0 \\ c_{off} & F \cdot (v_2 - v_1) < 0, (x_1 - x_2) \cdot (v_1 - v_2) \geq 0 \end{cases} \quad (15)$$

which can be simplified as

$$c_4 = \begin{cases} c_{off} & F \cdot (v_2 - v_1) \geq 0 \cap (x_1 - x_2) \cdot (v_1 - v_2) \geq 0 \\ c_{on} & F \cdot (v_2 - v_1) < 0 \cup (x_1 - x_2) \cdot (v_1 - v_2) < 0 \end{cases} \quad (16)$$

These two algorithms have different emphasis and both have its own advantages and disadvantages. Algorithm 1 only considers the energy changes of the elastic elements and damping elements between raft and unit, but doesn't take the change of the system total energy into account. Algorithm 2 concerns not only the absorption, release, and consumption of local energy, but also considers the change of the total energy of the system.

#### 4 SIMULATIONS AND ANALYSES

To verify the switch semi-active control algorithms, we simulated the floating raft vibration isolation system in MATLAB Simulink as shown in Fig. 7, and applied the control algorithms.

For comparison, the acceleration response of the foundation without control (including the off-state and the on state system) is also studied both in time domain and frequency domain analysis. The simulation parameters of the model are shown in Table 2, which is determined by the floating raft vibration isolation system used for tests.

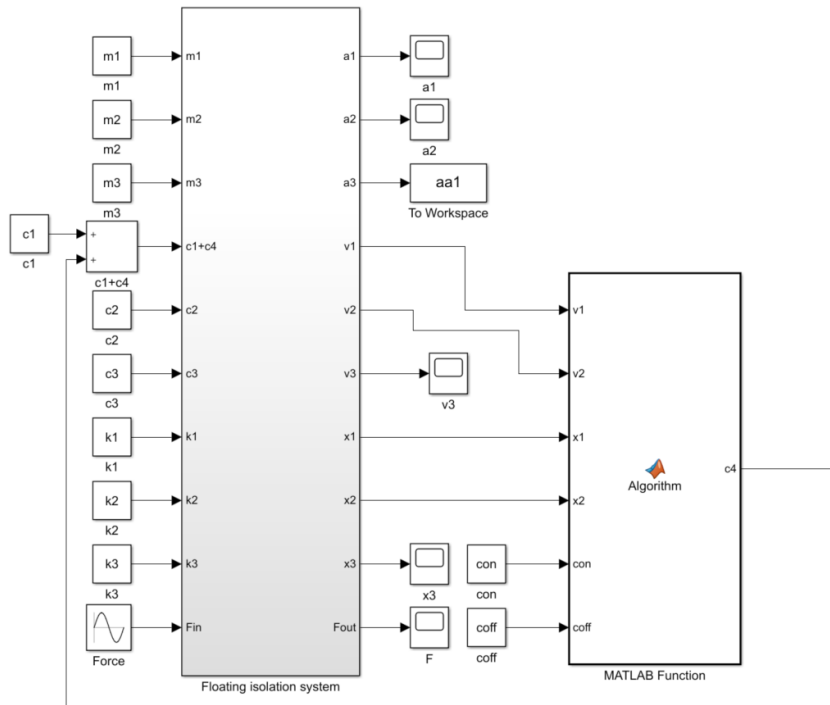


Fig. 7. Simulink model of the semi-active controlled floating raft isolation system

**Table 2.** Model parameters for semi-active controlled floating raft isolation system

Parameters	Value	
Equivalent mass [kg]	$m_1$	238.8
	$m_2$	175.1
	$m_3$	216
Equivalent damping [N·m <sup>-1</sup> ·s]	$c_1$	70
	$c_2$	50
	$c_3$	5000
Controllable damper [N·m <sup>-1</sup> ·s]	$c_{off}$	2100
	$c_{on}$	$4.81 \times 10^4$
Equivalent stiffness [N·m <sup>-1</sup> ]	$k_1$	$3.707 \times 10^5$
	$k_2$	$3.468 \times 10^5$
	$k_3$	$2.809 \times 10^7$

**4.1 Time Domain Comparison of Foundation Responses**

The amplitude of the excitation force acting on the unit in the simulation model is determined to be 500 N referring to the magnitude of the excitation force in the test device used in this study, and its frequency range is from 0.1 Hz to 20 Hz. As shown in Fig. 8, four typical frequencies were selected from the simulation results for analysis.

The first frequency (3.9 Hz) is the first resonance frequency of the non-controlled system. Fig. 8a shows that under the harmonic excitation of 3.9 Hz, the foundations of the systems controlled by

Algorithms 1 and 2 both have acceleration response amplitudes distinctly lower than that of the off-state system, higher than that of the on-state system and that from Algorithm 2 is even lower than Algorithm 1. These indicate that the vibration isolation effect of Algorithms 1 and 2 is obviously superior to that of the off-state system and is worse than that of the off-state system. The effect of Algorithm 2 is better than Algorithm 1 at this frequency .

The second frequency (4.7 Hz) is the frequency near the first resonance frequency under the control of the algorithms. Fig. 8b shows that under the harmonic excitation of 4.7 Hz, the foundations of the systems controlled by Algorithms 1 and 2 both have acceleration response amplitudes distinctly higher than that of the off-state system. These indicate that the isolation effect of the off-state system is superior to the Algorithms 1 and 2 at this frequency.

The third frequency (6.0 Hz) is the frequency where the effect with and without control are close. Fig. 8c shows that, under the harmonic excitation of 6 Hz, the foundations of the systems controlled by Algorithms 1 and 2 both have acceleration response amplitudes close to non-controlled system. These indicate that the isolation effect of non-control, Algorithms 1 and 2 is approximately equivalent at this frequency.

The last frequency (11 Hz) is the second resonance frequency of the non-controlled system. Fig. 8d shows that, under the harmonic excitation of

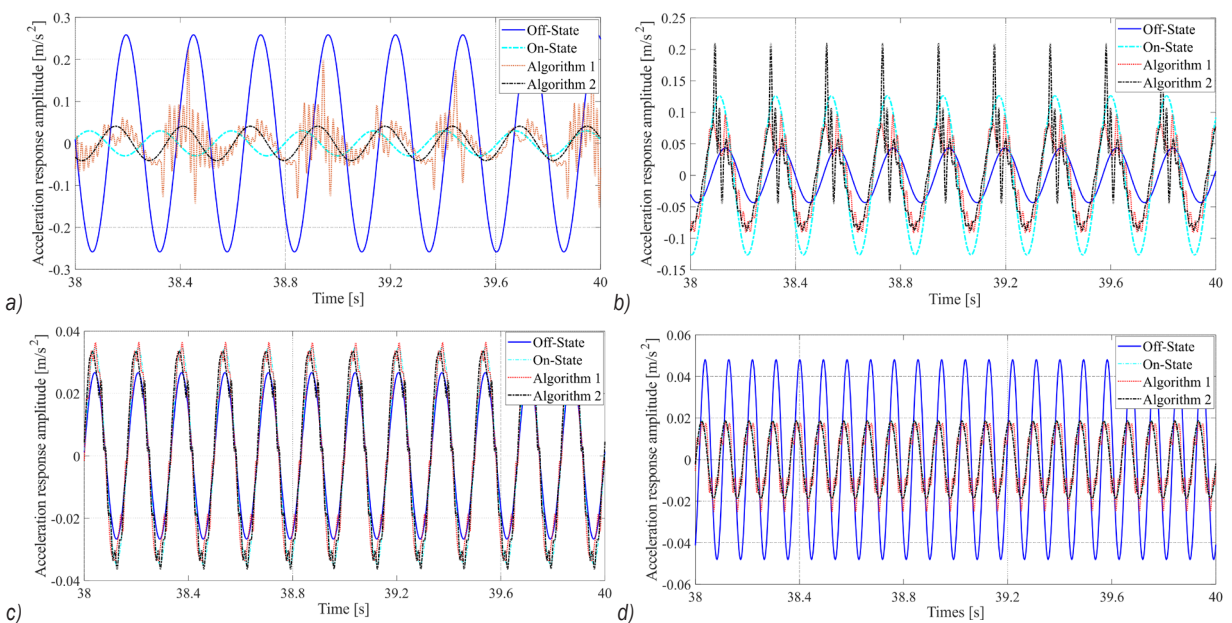


**Fig. 8.** Plot of acceleration response amplitude with respect to time; a) 3.9 Hz, b) 4.7 Hz, c) 6 Hz, and d) 11 Hz

11 Hz, the foundations of the systems controlled by Algorithms 1 and 2 both have acceleration response amplitudes distinctly lower than that of the off-state system. These indicate that the isolation effect of the off-state system is inferior to Algorithms 1 and 2; and there is little difference between the results of the on-state system, Algorithms 1 and 2, which suggest that the Algorithm 1 is basically in line with Algorithm 2 at this frequency.

#### 4.2 Frequency Domain Comparison of Foundation Responses

For the goal of comparison with the original system which has no switch-controllable damper, we carried out the frequency domain analysis of this case in additional. Continuously changing the frequency of the excitation force on the system and recording the foundation's acceleration response yields the variation curve of the acceleration response amplitude on the foundation of the system in the excitation frequency range from 0.1 Hz to 20 Hz, as shown in Fig. 9. There are two obvious resonance peaks in the response amplitude curve of the foundation acceleration of the original system.

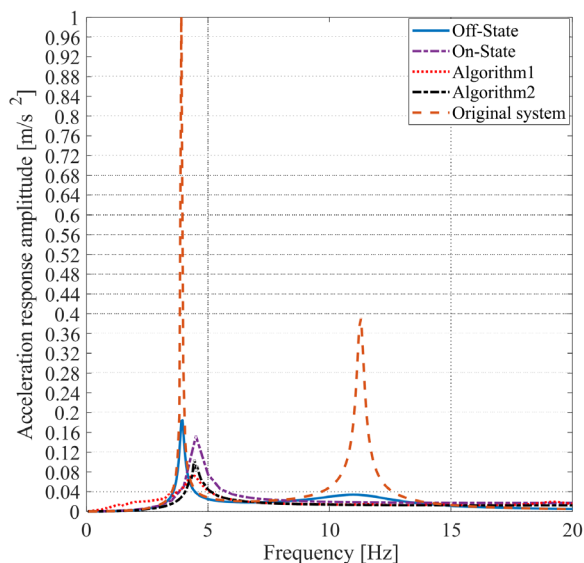


Fig. 9. Plot of acceleration response amplitude with respect to frequency obtained by simulation

According to Fig. 9, it can be seen that the trends of acceleration responses of the foundation of the four cases are basically similar, all of which reach the maximum at the resonance frequency. It is obvious that the acceleration response amplitude of the foundation of the original system is greatly

reduced after the installation of controllable damper. Comparing between systems using the controllable damper, the amplitudes of acceleration response on the foundation of the systems using two algorithms are significantly smaller than that of non-controlled system around the resonance frequency. Before reaching to the resonance frequency, the vibration isolation effect of Algorithm 1 is the worst while Algorithm 2 is the best; after the resonant frequency, the effect of these two algorithms are close to that of the non-controlled system. Compared with Algorithm 2, Algorithm 1 performs better around the resonance frequency but is inferior to Algorithm 2 in the low frequency band; in the following frequency band, the performance of two algorithms is approximately the same.

From the amplitude value of the foundation's acceleration response curve, the maximum values of the original system, the off-state system, the on-state system and the system using Algorithms 1 and 2 are shown in Table 3. The amplitude of the Original system is much larger and thus the vibration isolation effect is poorer; and the vibration isolation effect gets better when the controllable damper is used. Compared with non-controlled system, the amplitude of the system using Algorithm 1 is reduced by 60.4 %, and using Algorithm 2 is reduced by 43.3 %; the amplitude using Algorithm 1 is reduced by 30.1 % compared with that using Algorithm 2.

Table 3. Acceleration response maximum of five states (simulation)

State	Maximum [m/s <sup>2</sup> ]
Original system	1.012
Off-State	0.1844
On-State	0.1526
Algorithm 1	0.07296
Algorithm 2	0.1045

It can be concluded that using controllable damper can improve the isolation effect of the floating raft isolation system in the low frequency segment; furthermore, using the algorithms to control the controllable damper can further improve the vibration isolation effect.

## 5 EXPERIMENTS

### 5.1 Test System and Scheme

We built the experiment setup for the semi-active controlled floating raft vibration isolation system, which consists of a floating raft vibration test bench, a

switch-controller system, and a test evaluation system. The block diagram is shown in Fig. 10.

The floating raft vibration test bench is composed of a unit, a variable-frequency drive (VFD), upper isolation springs, a raft, lower isolation springs,

foundation, and controllable dampers. The switch-controller system is composed of acceleration sensors, conditioning amplifier, PCI DAQ, Industrial Personal Computer (IPC) and a relay. The velocities and displacements needed in the algorithms can be

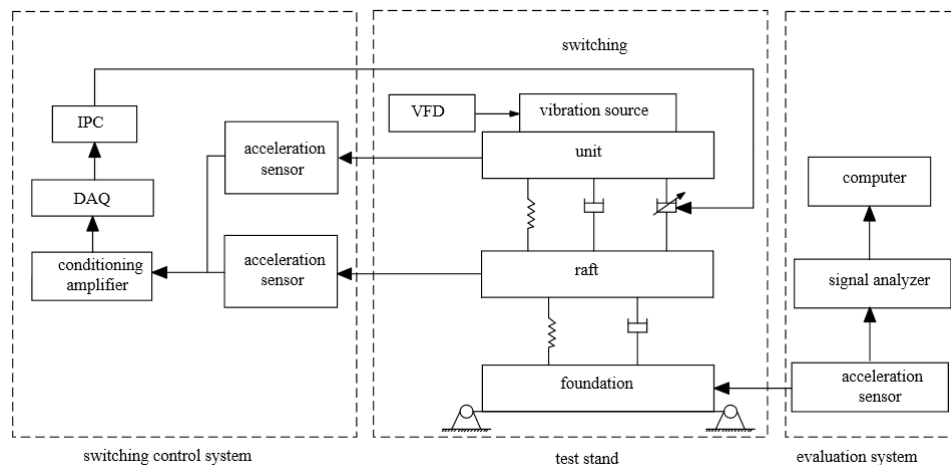


**Fig.10.** Test block diagram of semi-active control of floating raft isolation system

obtained from integration. The test evaluation system has composed of 333B30 acceleration sensors (PCB Piezotronics, Inc., USA) and a Siglab20-42 signal analyser (Spectral Dynamic, Inc., USA), Siglab analysis software is installed on the computer.

The variable-frequency drive controls the excitation force on the unit to generate harmonic excitation at different frequencies. The switch semi-active control algorithms are implemented by running the control program of LabVIEW. It switches the controllable damper by controlling the relay. The test evaluation system collects the acceleration response signals on the foundation for analysis. This setup of the experiment is shown in Fig. 11.



**Fig. 11.** The experimental apparatus

## 5.2 Results and Analysis

We tested the original system, the non-controlled system (the On-State or Off-State system), and the semi-active switch-controlled systems using Algorithms 1 and 2, respectively, from which the variation curves of the acceleration response amplitudes of the foundations at the excitation frequency range from 1.5 Hz to 13 Hz are obtained, as shown in Fig. 12.

From the amplitude value of the foundation's acceleration response curve, the maximum values of the original system, Off-state system, On-state system, Algorithms 1 and 2 are obtained and shown in Table 4. The vibration isolation effect of the original system is not obvious. Acceleration response amplitudes of the original system, the off-state system, the on-state system, the semi-active switch-controlled systems using Algorithms 1 and 2, respectively, are 0.0573, 0.02243, 0.1826, 0.01127 and 0.01321.

Comparing Figs. 9 and 12, it can be seen that the simulation results are in good agreement with the experimental results. Around the resonance frequency, the vibration isolation effect of semi-active control using Algorithms 1 and 2 is clearly better than that of non-controlled system, and they are roughly the same at other frequencies, which shows that Algorithms 1 and 2 can effectively improve the vibration isolation

performance of floating raft system around the resonance frequency.

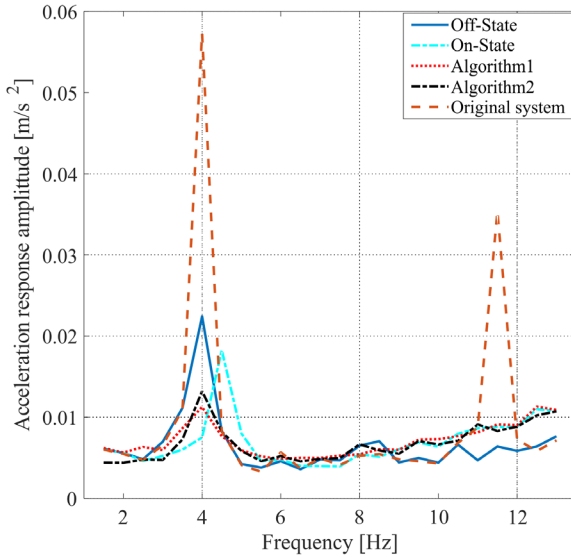


**Fig. 12.** Plot of acceleration response amplitude with respect to frequency obtained by experiment test

**Table 4.** Acceleration response maximum of three states (test)

State	Maximum [m/s <sup>2</sup> ]
Original system	0.0573
Off-State	0.02243
On-State	0.01826
Algorithm 1	0.01127
Algorithm 2	0.01321

It is worth mentioning that there are some discrepancies in the magnitude of the underlying acceleration between simulation and testing.

- Compared with the simulation results, the basic acceleration amplitude of the test generally increases gradually with the increase of the frequency. The reason for this is that the test system adopts an inertial rotation excitation device, and the amplitude of the excitation force gradually increases with the increase of the frequency (i.e., the rotation speed), while the constant amplitude excitation force is used in the simulation model.
- In the test results, the frequencies corresponding to the first-order peaks are basically the same except for the open state of the damper. In the open state of the damper, the frequency increases slightly. In the simulation results, however, the frequency increases in the on state and two control algorithm states compared to the off and original system states. The main reason for this discrepancy is

that the properties and values of all damping of the actual floating raft vibration isolation system are very complex, and the damping force can be understood as the superposition of damping forces of various properties. In the simulation model, only the viscous damping of the system is considered, which makes the damping in the simulation model relatively small. The main influencing factor of the frequency corresponding to the first-order peak is the system damping ( $c_1 + c_4$ ). When ( $c_1 + c_4$ ) is larger, the frequency corresponding to the first-order peak is also larger. Since the parameter  $c_1$  in the test system is larger than the parameter in the simulation model, in the vicinity of the first-order peak frequency, after the algorithm is applied to the test system, the larger  $c_1$  makes  $c_4$  do not need to be turned on frequently, and the switch damper  $c_4$  is in the off state as the dominant factor. The damping ( $c_1 + c_4$ ) in the test system is more in a less damped state and the frequency corresponding to the first-order peak barely increases. After the simulation model applies the algorithm, the smaller  $c_1$  makes  $c_4$  need to be turned on frequently, and the switch damper  $c_4$  is in the on state as the dominant factor. The damping ( $c_1 + c_4$ ) in the simulation model is more in the larger damping state and the frequency corresponding to the order peak increases slightly.

In addition, we only consider the viscous damping of the floating raft system in the simulation model and the amplitude of the second peak in the simulation results decreases as the damping increases. In the actual test system, when the controllable damper is in the off state, the characteristics of damping ( $c_1 + c_4$ ) mainly depend on  $c_1$ , and the non-viscous damping characteristics become obvious, which leads to the discrepancies between the experimental results (the amplitude of the second peak is small) and the simulation results.

## 6 CONCLUSIONS

To solve the problem that the vibration isolation effect of the floating raft vibration isolation system is poor near the resonance frequency and even has a vibration amplification effect, we developed a switch-controllable damper and introduced semi-active switch control technology. Two switch control algorithms, Algorithms 1 and 2, are proposed. Based on the simulation and experiments, the following conclusions can be drawn:

- (1) The controllable damper can improve the isolation effect of the vibration isolation system near the resonance frequency. Built on that, the vibration isolation effect of the system can be further greatly improved by using the proposed semi-control algorithms.
- (2) The two control algorithms have their own advantages and disadvantages. In the low frequency band, the overall isolation effect of Algorithm 2 is better than that of Algorithm 1. However, near resonance frequency, using Algorithm 1 in the vibration isolation effect is more superior near the resonance frequency.
- (3) Future work on this can be carried out in the direction of multi-frequency excitation, which is closer to the practical engineering application.

## 7 REFERENCES

- [1] He, L., Xu, W. (2013). Naval vessel machinery mounting technology and its recent advances. *Acta Acustica*, vol. 38, no. 2, p. 128-136, DOI:10.15949/j.cnki.0371-0025.2013.02.001. (in Chinese)
- [2] Niu, J., Song, K., Lim, C.W. (2005). On active vibration isolation of floating raft system. *Journal of Sound and Vibration*, vol. 285, no. 1-2, p. 391-406, DOI:10.1016/j.jsv.2004.08.013.
- [3] Wang, Z., Mak, C.M. (2018). Application of a movable active vibration control system on a floating raft. *Journal of Sound and Vibration*, vol. 414, p. 233-244, DOI:10.1016/j.jsv.2017.11.026.
- [4] Fuller, C.R., Elliott, S.J., Nelson, P.A. (1997). Active control of vibration. *Physics Today*, vol. 50, no. 5, p. 64, DOI:10.1063/1.881838.
- [5] Liu, Y., Shu, Y., Hu, W., Zhao, X., Xu, Z. (2021). Active vibration control of a mechanical servo high-speed fine-blanking press. *Strojniški vestnik - Journal of Mechanical Engineering*, vol. 67, no. 9, p. 445-457, DOI:10.5545/sv-jme.2020.6959.
- [6] Ghiringhelli, G.L. (2000). Testing of semiactive landing gear control for a general aviation aircraft. *Journal of Aircraft*, vol. 37, no. 4, p. 606-616, DOI:10.2514/2.2672.
- [7] Jung, H.-J., Park, K.-S., Spencer, B.F.Jr, Lee, I.-W. (2010). Hybrid seismic protection of cable-stayed bridges. *Earthquake Engineering & Structural Dynamics*, vol. 33, no. 7, p. 795-820, DOI:10.1002/eqe.374.
- [8] Sun, H.L., Zhang, K., Zhang, P.Q., Chen, H.B. (2010). Application of dynamic vibration absorbers in floating raft system. *Applied Acoustics*, vol. 71, no. 3, p. 250-257, DOI:10.1016/j.apacoust.2009.09.005.
- [9] Gao, X., Fan, G., Jin, C., Dong, G. (2016). Double-layer vibration suppression bilinear system featuring electro-rheological damper with optimal damping and semi-active control. *Journal of Vibroengineering*, vol. 18, no. 6, p. 3891-3914, DOI:10.21595/jve.2016.16577.
- [10] Zhao, C., Chen, D. (2008). A two-stage floating raft isolation system featuring electrorheological damper with semi-active fuzzy sliding mode control. *Journal of Intelligent Material Systems and Structures*, vol. 19, no. 9, p. 1041-1051, DOI:10.1177/1045389X07083141.
- [11] Hamme, R.N. (1956). Acoustical materials problems posed by low-frequency sound control. *Noise Control*, vol. 2, no. 5, p. 10, DOI:10.1121/1.2369224.
- [12] Sykes, A.O. (1960). Isolation of vibration when machine and foundation are resilient and when wave effects occur in the mount. *Noise Control*, vol. 6, p. 23-38, DOI:10.1121/1.2369414.